Received: 10 May 2018 | Accepted: 15 November 2018

DOI: 10.1002/hyp.13352

RESEARCH ARTICLE

WILEY

# Alternative analysis of transient infiltration experiment to estimate soil water repellency

Vincenzo Alagna[1] | Massimo Iovino[1] | Vincenzo Bagarello[1] | Jorge Mataix-Solera[2] | Lubomir Lichner[3]

[1] Dipartimento di Scienze Agrarie, Alimentari e Forestali, Università degli Studi di Palermo, Palermo, Italy

[2] Departamento de Agroquímica y Medio Ambiente, Universidad Miguel Hernández, Elche, Spain

[3] Institute of Hydrology, Slovak Academy of Sciences, Bratislava, Slovak Republic

**Correspondence**
Massimo Iovino, Dipartimento di Scienze Agrarie, Alimentari e Forestali, Università degli Studi di Palermo, Palermo, Italy.
Email: massimo.iovino@unipa.it

**Funding information**
Università degli Studi di Palermo, Grant/Award Number: D50002D13+1012; Montgó Natural Park; Botánica Mediterránea S.L.; Ministerio de Economía and Competitividad of Spanish Government, Grant/Award Number: CGL2013-47862-C2-1-R; Slovak Research and Development Agency APVV, Grant/Award Number: APVV-15-0160; Ministero dell'Istruzione, dell'Università e della Ricerca, Grant/Award Number: B72F16000550005

## Abstract

The repellency index (RI) defined as the adjusted ratio between soil-ethanol, $S_e$, and soil-water, $S_w$, sorptivities estimated from minidisk infiltrometer experiments has been used instead of the widely used water drop penetration time and molarity of ethanol drop tests to assess soil water repellency. However, sorptivity calculated by the usual early-time infiltration equation may be overestimated as the effects of gravity and lateral capillary are neglected. With the aim to establish the best applicative procedure to assess RI, different approaches to estimate $S_e$ and $S_w$ were compared that make use of both the early-time infiltration equation (namely, the 1 min, S1, and the short-time linearization approaches), and the two-term axisymmetric infiltration equation, valid for early to intermediate times (namely, the cumulative linearization and differentiated linearization approaches). The dataset included 85 minidisk infiltrometer tests conducted in three sites in Italy and Spain under different vegetation habitats (forest of *Pinus pinaster* and *Pinus halepensis*, burned pine forest, and annual grasses), soil horizons (organic and mineral), postfire treatments, and initial soil water contents. The S1 approach was inapplicable in 42% of experiments as water infiltration did not start in the first minute. The short-time linearization approach yielded a systematic overestimation of $S_e$ and $S_w$ that resulted in an overestimation of RI by a factor of 1.57 and 1.23 as compared with the cumulative linearization and differentiated linearization approaches. A new repellency index, $RI_s$, was proposed as the ratio between the slopes of the linearized data for the wettable and hydrophobic stages obtained by a single water infiltration test. For the experimental conditions considered, $RI_s$ was significantly correlated with RI and WDPT. Compared with RI, $RI_s$ includes information on both soil sorptivity and hydraulic conductivity and, therefore, it can be considered more physically linked to the hydrological processes affected by soil water repellency.

**KEYWORDS**

infiltration, minidisk infiltrometer, repellency index, soil hydraulic conductivity, soil sorptivity, soil water repellency, two-term infiltration model, water drop penetration time

## 1 | INTRODUCTION

Soil water repellency (SWR) reduces affinity of soils to water resulting in detrimental implication for plant growth as well as for hydrological processes. These include reduced matrix infiltration, development of fingered flow, irregular wetting fronts, and overall increased runoff generation and soil erosion (DeBano, 2000; Doerr, Shakesby, & Walsh, 2000). During the last decades, it has become clear that SWR is much

 © 2018 John Wiley & Sons, Ltd. 

more widespread than formerly thought, having been reported for a wide variety of soils, land uses, and climatic conditions (Dekker, Oostindie, & Ritsema, 2005). SWR stems from reorientation of amphiphilic compounds during heating or drying, which results in a nonzero contact angle between water and soil. In severe cases, when the contact angle exceeds 90°, water infiltration is prevented (Letey, Carrillo, & Pang, 2000). However, it has increasingly been recognized that infiltration rates and pattern can be affected by *subcritical* repellency that occurs when the water-solid contact angle is less than 90° but not zero (Tillman, Scotter, Wallis, & Clothier, 1989). Under these circumstances, water infiltration rate is reduced but not prevented at all, as in the case of severe hydrophobicity (Hunter, Chau, & Si, 2011).

Due to its dynamic nature, including dependence on the initial soil water content, testing of SWR should be conducted directly under field-moist samples (Dekker, Ritsema, Oostindie, Moore, & Wesseling, 2009). The water drop penetration time (WDPT) test (Doerr, 1998; Letey et al., 2000; Watson & Letey, 1970) has been diffusely applied to assess the persistence of SWR. However, WDPT is a measure of the time required for the contact angle to change from its original value, which can be greater than 90°, to a value approaching 90° (Cerdà & Doerr, 2007; Letey et al., 2000). Given the wettability of a hydrophobic soil surface can be increased by lowering the surface tension of the liquid, the severity of SWR can be assessed by using different mixtures of water and ethanol. With the molarity of an ethanol droplet (MED) test, the severity of SWR is associated to the concentration (or liquid–air surface tension) of the aqueous ethanol solution that enters the soil in approximately 5 s (Letey et al., 2000). However, the MED test can only be used to determine apparent contact angles >90° and thus only to discriminate between critical and subcritical SWR (Carrillo, Yates, & Letey, 1999; Müller et al., 2016). Independently of the considered test (i.e., WDPT or MED), the soil surface area sampled in a drop scale infiltration test is of the order of 0.14 $cm^2$ and SWR assessment can be significantly influenced by spatial variability (Moody & Schlossberg, 2010).

Tillman et al. (1989) proposed a repellency index, RI, to assess subcritical SWR that basically is a measure of the reduced soil water sorptivity compared with a nonrepellent soil. Given ethanol readily infiltrates into hydrophobic soil, its sorptivity provides a measure of liquid transport in soil that is not influenced by SWR and is representative of pore structure (Orfánus et al., 2014). RI is defined as the ratio between soil-ethanol, $S_e$, and soil-water, $S_w$, sorptivities adjusted to account for the different surface tensions and viscosities of the two infiltrating liquids ($RI = 1.95 \cdot S_e/S_w$; Tillman et al., 1989). Iovino et al. (2018) proposed a classification of RI similar to that for WDPT with five classes of repellency considered: wettable ($RI \leq 1.95$), slightly water repellent ($1.95 \leq RI < 10$), strongly water repellent ($10 \leq RI < 50$), severely water repellent ($50 \leq RI < 110$), and extremely water repellent ($RI \geq 110$). Compared with drop scale infiltration tests, RI is determined from infiltration tests conducted at a larger scale and, thus, take into account soil properties and conditions (e.g., initial soil moisture, geometry, and connectivity of pores) that directly influence the effects of SWR on hydrological processes. Tension infiltration experiments are preferred to ponded ones to exclude the contribution of macropores that may overwhelm soil hydrophobicity (Ebel, Moody, & Martin, 2012; Nyman, Sheridan, & Lane, 2010). Miniaturized tension infiltrometers were proposed to determine SWR at the aggregate scale (Hallett & Young, 1999), but, for field use, standard infiltrometers are more suited. Hunter et al. (2011) compared the influence of tension infiltrometer disk size on the measured RI values and concluded that the minidisk infiltrometer (MDI; Decagon Devices Inc., Pullman, USA), having a 4.5-cm-diameter disk, is appropriate for field assessment of RI. In a recent investigation, the MDI proved to be a practical alternative to the classical tension infiltrometer to estimate hydrodynamic properties of a loam soil (Alagna, Bagarello, Di Prima, & Iovino, 2016).

Soil sorptivity, $S_0$ ($L/T^{0.5}$), is commonly estimated from the Philip (1957) horizontal infiltration equation, but the assessment of the linear part of cumulative infiltration, $I$ (L), versus square root of time, $t$ (T), relationship describing the early stage of the infiltration process could be relatively problematic in water repellent soils (Carrick, Buchan, Almond, & Smith, 2011; Di Prima, Lassabatere, Bagarello, Iovino, & Angulo-Jaramillo, 2016). Sorptivity was estimated as the infiltration rate out of a MDI during a fixed time interval, generally 1–5 min (Hunter et al., 2011; Lewis, Wu, & Robichaud, 2006; Robichaud, Lewis, & Ashmun, 2008), as it is considered fast enough to be an operational procedure for teams working in the field. However, the early-time linear regression of the $I$ versus $\sqrt{t}$ data neglects the effects of gravity and lateral capillary flux at the edge of the source thus resulting in $S_0$ overestimation (Angulo-Jaramillo, Bagarello, Iovino, & Lassabatere, 2016). An unbiased estimation of soil sorptivity is possible by fitting the two-term cumulative infiltration equation proposed by Haverkamp, Ross, Smettem, and Parlange (1994) to the infiltration data collected from early to intermediate infiltration times. In this case, validity of Philip's equation is not needed (Bagarello & Iovino, 2003; Vandervaere, Vauclin, & Elrick, 2000a). The Haverkamp et al. (1994) model has been largely applied to estimate the hydrodynamic properties of a variety of soils using infiltration data collected under both tension and ponded conditions (Bagarello, Di Prima, Iovino, & Provenzano, 2014; Dohnal, Dusek, & Vogel, 2010; Gonzalez-Sosa et al., 2010). However, to the best of our knowledge, the two-term infiltration model has never been applied to assess SWR.

Determination of the repellency index needs two sorptivity values, one for water and the other for ethanol, to be determined. As a consequence of the influence of the initial soil water content on both ethanol and water sorptivity (Tillman et al., 1989), the two experiments cannot be conducted at exactly the same spot. Due to both horizontal and vertical spatial variability of SWR (e.g., Dekker, Doerr, Oostindie, Ziogas, & Ritsema, 2001), a large number of replicated runs should be carried out to obtain a reliable estimate of the repellency index, for a given area, by the ratio of the averages of sorptivity found with ethanol and water. The possibility to derive a repellency index from a unique water infiltration experiment conducted by the MDI at a single spot is thus intriguing, also considering the potential advantages that stem from the simplicity of the technique (portability, small volumes of water, and short duration of field experiment). An attempt to assess SWR by a single experiment was made by Lichner et al. (2013), who defined the water repellency cessation time (WRCT) as the time corresponding to the intersection of the two straight lines representing the $I$ versus $\sqrt{t}$ relationship for hydrophobic and near wettable conditions. Alagna, Iovino, Bagarello, Mataix-Solera, and Lichner (2017) found that the WRCT was significantly correlated to WDPT and concluded that

WRCT is essentially a measure of the persistence of SWR. However, the potentiality of a single water infiltration experiment conducted with the MDI to provide information on the SWR still needs investigation also because water repellent and wettable soils could show qualitatively similar behaviours when infiltration data are reported on a $I$ versus $\sqrt{t}$ plot (Cook & Broeren, 1994; Smettem, Parlange, Ross, & Haverkamp, 1994).

The general objective of this study was to strengthen the techniques for assessing SWR from tension infiltration experiments conducted in the field by the MDI. In particular, with the aim to establish the best applicative procedure to estimate the classical water repellency index according to Tillman et al. (1989), different techniques to calculate the soil sorptivity using ethanol, $S_e$, and water, $S_w$, were compared including (a) infiltration rate in a fixed time interval, (b) analysis of early-time infiltration data, and (c) linearization of the axisymmetric transient infiltration equation. With the aim to simplify SWR assessment, a new repellency index, obtained from a unique water infiltration test, was proposed and evaluated with existing approaches. Three Mediterranean sites under various soil/vegetation/management conditions were considered to evaluate the different procedures for estimating SWR.

## 2 | THEORY

Haverkamp et al. (1994) proposed the following three-dimensional infiltration equation for disk infiltrometers, valid for short to medium times:

$$I = S_0\sqrt{t} + \left[\frac{2-\beta}{3}K_0 + \frac{\gamma S_0^2}{r(\theta_0 - \theta_i)}\right]t, \quad (1)$$

where $I$ (L) is the cumulative infiltration; $t$ (T) is the infiltration time; $\theta_0$ ($L^3/L^3$) is the volumetric soil water content corresponding to the imposed pressure head at the soil surface, $h_0$ (L); $\theta_i$ ($L^3/L^3$) is the initial volumetric soil water content; $S_0 = S(h_0)$ ($L/T^{1/2}$) is the soil sorptivity; $K_0 = K(h_0)$ (L/T) is the soil hydraulic conductivity; $r$ (L) is the radius of the disk source; and β and γ are coefficients that are commonly set at 0.6 and 0.75, respectively. The first term of the right-hand side of Equation 1 accounts for vertical capillary flow and dominates infiltration during its early stage. The second term corresponds to the gravity-driven vertical flow, and the third one represents the lateral capillary component at the edge of the circular infiltration surface (Smettem et al., 1994).

Equation 1 can be linearized by dividing both sides by $\sqrt{t}$ (cumulative linearization [CL] method) or by differentiating the cumulative infiltration data with respect to the square root of time (differentiated linearization [DL] method; Vandervaere et al., 2000a). In both cases, the soil sorptivity can be estimated as the intercept of the regression line fitted to the linearized experimental data. With this approach, the effects of gravity and lateral expansion are explicitly accounted for and soil sorptivity can be obtained using the complete experimental information collected for short to medium time (Angulo-Jaramillo et al., 2016). Vandervaere, Vauclin, and Elrick (2000b) proposed the DL method to account for the water stored in the contact material during the early stages of infiltration. However, if no contact material is used, the CL and DL methods should result in similar $S_0$ estimates. A test of the expected equivalence of the two methods was conducted by Bagarello and Iovino (2004), who found that the two linearization methods were not perfectly equivalent in estimating $S_0$. When the experimental cumulative infiltration data are plotted in the form of $I/\sqrt{t}$ versus $\sqrt{t}$ or $dI/d\sqrt{t}$ versus $\sqrt{t}$, the validity of Equation 1 can easily be checked and discontinuities in the infiltration process can easily be detected given they result in deviation from the monotonically increasing linear behaviour (Vandervaere et al., 2000a). Water repellency is one of most common circumstances producing deviation from the classical infiltration theory (Di Prima et al., 2016; Ebel & Moody, 2013; Imeson, Verstraten, van Mulligen, & Sevink, 1992).

In water repellent soils, infiltration rate can be expected to increase, after an initial stage at null or low values, as a consequence of soil wetting (Beatty & Smith, 2013; Carrick et al., 2011). Therefore, comparing the soil hydrodynamic data collected during the initial hydrophobic and subsequent wetting stages of an infiltration process potentially allows us to quantify SWR. In particular, provided Equation 1 can separately be applied to both stages, the extent of water repellency can be defined as the ratio, $RI_s$, between the slopes of the linearized cumulative infiltration relationships fitting the hydrophobic and wetting stages of the infiltration process corresponding to an imposed $h_0$ value:

$$RI_s = \frac{\left[\frac{2-\beta}{3}K_{ws} + \frac{\gamma S_{ws}^2}{r\Delta\theta}\right]}{\left[\frac{2-\beta}{3}K_{rs} + \frac{\gamma S_{rs}^2}{r\Delta\theta}\right]}, \quad (2)$$

in which the subscript *ws* refers to the wetting stage of infiltration, the subscript *rs* refers to the repellent stage, and $\Delta\theta = \theta_0 - \theta_I$ (Figure 1). For wettable soils a value $RI_s = 1$ is expected.

Compared with repellency indices that make use of two sorptivity measurements conducted with ethanol and water at two different sites, the repellency index defined by Equation (2) needs only one

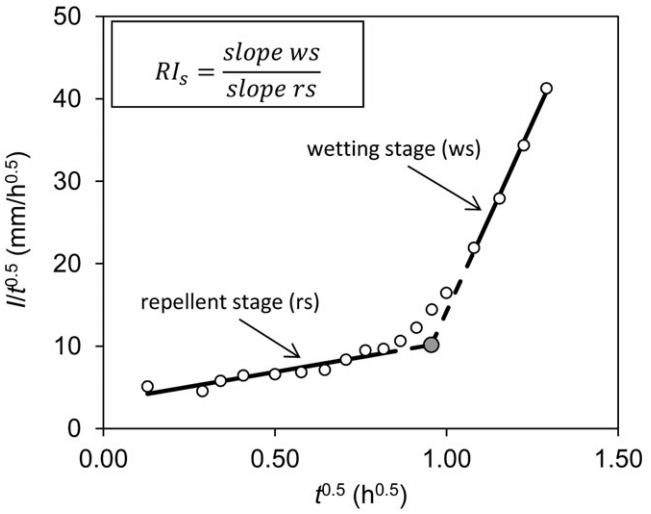


**FIGURE 1** Selection of the water repellent and wetting stages from linearized infiltration data (cumulative linearization method)

infiltration experiment with water at a single spot and it accounts for the effects induced by water repellency on the two hydrodynamic properties (sorptivity and hydraulic conductivity) that directly influence the hydrological processes.

## 3 | MATERIALS AND METHODS

### 3.1 | Field sites

Infiltration data were collected in the two Mediterranean managed pine forests of Ciavolo (Italy) and Javea (Spain), already investigated by Alagna et al. (2017), and in the fire-affected forest site of Javea, in which different postfire management strategies were implemented. Soil at Ciavolo site is a *Typic Rhodoxeralf* (Soil Survey Staff, 2014), and the forest consists of 30 years old *Pinus pinaster* trees. Measurements were conducted on both the approximately 5-cm-thick decomposed organic floor layer (duff) and the underlying mineral soil layer 2 times in 2014 (in summer and autumn) to explore different moisture conditions (Alagna et al., 2017). Indeed, influence of initial soil moisture on water repellency is well recognized in literature (i.e., de Jonge, Jacobsen, & Moldrup, 1999; Dekker et al., 2001; Vogelmann et al., 2013). Between the two measurement times, 108 mm of rainfall occurred that is approximately 20% of the average annual precipitation for the location. For comparative purposes, a glade area vegetated with spontaneous annual grasses (*Avena fatua* L., *Galactites elegans* [All.] Soldano, *Hypochaeris achyrophorus* L., *Oxalis pes-caprae* L., and *Vulpia ciliata* Dumort) was also sampled, approximately 50 m away from the pine site, at the second measurement time. Only the surface mineral layer was sampled at this site given that a well-developed organic layer was not detectable. Average air temperature on the two sampling dates was 24.7 and 18.2°C, respectively.

The second measurement site is located at Javea close to Alicante, Spain, in a 40-year-old afforested plantation of *Pinus halepensis* that was settled on abandoned agricultural terraces. The soil is *Lithic Rhodoxeralf* (Soil Survey Staff, 2014) developed over a karstified limestone. Measurements were conducted in the beginning of July 2015 at the surface duff and the underlying mineral soil layer. The mean air temperature at the time of measurements was 26.5°C, and no rainfall had occurred in the 3 months prior to sampling, thus resulting in relatively dry initial soil moisture conditions.

The third site was also located at Javea in an area that was fire-affected in September 2014 resulting in a complete loss of forest trees. Starting from December 2014, the following two alternative postfire management strategies were implemented in this area: (a) burned trees were cut at the ground level and removed (cutting treatment, C) and (b) the soil was mulched with chopped pine residues (residue treatment, R). For comparative purposes, a control plot (no treatment, N), in which no operation was performed and the burned vegetation was left in situ, was also considered. Field measurements at the three plots of the fire-affected site were performed on 15–17 June 2015. Only the soil mineral layer was sampled after removing ash and/or mulching residues. The mean daily temperature at the time of sampling was 20.8° C. Characteristics of experimental sites were summarized in Table 1.

For the aim of comparisons among repellency indices calculated by the different procedures, 10 experimental conditions were therefore considered resulting from different habitats (i.e., *Pinus pinaster* forest in Ciavolo [P], spontaneous annual grasses in Ciavolo [G], *Pinus halepensis* forest in Javea [H], and burned pine forest in Javea [B]), sampled horizons (i.e., organic [O] or mineral [M]), climatic conditions at the vegetated sites (i.e., dry [D] or wet [W] season), and postfire treatments at the fire-affected site (no treatment [N], cutting treatment [C], and residues treatment [R]). Each experimental condition is therefore identified by three capital letters indicating, respectively, habitat, sampled horizon, and soil moisture at the time of sampling or postfire treatment.

### 3.2 | Field measurements

For each experimental condition, a flat area (approximately 5 × 5 $m^2$) was selected and scrubbed soil samples were randomly collected in the first 5 cm of each sampled horizon to determine particle size distribution, using the hydrometer method (Gee & Bauder, 1986), and organic matter content by the Walkley-Black method (Nelson & Sommers, 1996). The clay, silt, and sand percentages were determined, as a mean of three replicated samples, according to U.S. Department of Agriculture standards (Table 1). Undisturbed soil cores were randomly collected by gently pressing stainless steel cylinders (0.05 m in height by 0.05 m in diameter) into the sampled soil layer to determine soil bulk density, $\rho_b$ ($Mg/m^3$), and volumetric water content at the time of sampling, $\theta_i$ ($m^3/m^3$) (Table 2).

**TABLE 1** Characteristics of the investigated sites

| Site | Coordinates UTM | Elevation and slope | Land use | Soil type | Clay (%) | Silt (%) | Sand (%) | Soil texture (USDA) |
|---|---|---|---|---|---|---|---|---|
| Ciavolo, Marsala (Italy) | 37°45′19.2″N, 12°33′53.5″E | 105 m asl 4.4% | *Pinus pinaster* (30 years old), | *Typic Rhodoxeralf* | 33.4 | 43.0 | 23.6 | Clay-loam |
| Ciavolo, Marsala (Italy) | 37°45′19.6″N, 12°33′58.1″E | 105 m asl 4.4% | Spontaneous annual grasses | *Typic Rhodoxeralf* | 28.5 | 34.5 | 39.6 | Clay-loam |
| Javea, Alicante (Spain) | 38°48′10.6″N 0°11′23.4″E | 98 m asl 0% | *Pinus halepensis* (40 years old) | *Lithic Rhodoxeralf* | 40.8 | 43.3 | 15.7 | Silty-clay |
| Javea, Alicante (Spain) | 38°48′15.0″N 0°09′18.8″E | 213 m asl 5% | Burned pine forest under different post-fire treatments | *Lithic Rhodoxeralf* | 11.1 | 34.8 | 54.1 | Sandy-loam |

*Note*. USDA, U.S. Department of Agriculture.

**TABLE 2** Means and coefficients of variation (CV) of initial soil water content, $\theta_i$; bulk density, $\rho_b$; organic matter content, OM; and Water Drop Penetration Time, WDPT, for the experimental conditions considered resulting from different vegetation habitat (P, *Pinus pinaster* forest; H, *Pinus halepensis* forest; B, burned pine forest; G, glade), soil sampled horizon (O, organic soil; M, mineral soil), initial soil moisture condition (i.e., dry [D] or wet [W]), and postfire treatment (no treatment [N], cutting treatment [C], and residues treatment [R])

| Experimental condition | $\theta_i$ (cm $^3$/cm$^3$) | | | $\rho_b$ (g/cm$^3$) | | | OM (%) | | | WDPT (s) | | | |
|---|---|---|---|---|---|---|---|---|---|---|---|---|---|
| | *N* | mean | CV (%) | *N* | mean | CV (%) | *N* | mean | CV (%) | *N* | geometric mean | CV (%) | Range |
| P-O-D | 10 | 0.128 | 16.9 | 10 | 0.725 | 32.4 | 10 | 20.0 | 7.04 | 30 | 1689 | 48 | 868–3534 |
| P-O-W | 10 | 0.175 | 8.01 | 10 | 0.749 | 9.50 | 10 | 21.5 | 1.07 | 30 | 1454 | 182 | 150–6890 |
| P-M-D | 9 | 0.166 | 6.33 | 9 | 1.172 | 4.14 | 10 | 4.66 | 2.41 | 29 | 300 | 54 | 113–855 |
| P-M-W | 10 | 0.169 | 5.80 | 10 | 1.089 | 5.70 | 10 | 3.93 | 3.11 | 30 | 745 | 137 | 100–4425 |
| G-M-W | 10 | 0.281 | 7.51 | 10 | 1.192 | 4.73 | 10 | 4.71 | 6.02 | 29 | <5 | - | - |
| H-O-D | 10 | 0.066 | 36.9 | 10 | 0.548 | 45.5 | 10 | 26.6 | 12.6 | 30 | 2139 | 116 | 480–7517 |
| H-M-D | 8 | 0.098 | 29.2 | 8 | 1.082 | 14.9 | 10 | 8.54 | 3.83 | 29 | 5 | 106 | 1–18 |
| B-M-N | 5 | 0.046 | 39.9 | 5 | 1.025 | 12.6 | 9 | 7.70 | 14.6 | 30 | 90 | 238 | 8–2220 |
| B-M-C | 5 | 0.020 | 19.3 | 5 | 0.876 | 19.4 | 9 | 6.73 | 13.6 | 30 | 45 | 951 | 5–1800 |
| B-M-R | 5 | 0.034 | 15.3 | 5 | 1.011 | 8.00 | 9 | 7.15 | 9.55 | 30 | 27 | 683 | 5–1200 |

*Note*. Range between minimum and maximum values for WDPT is also given.

The WDPT test was carried out under field moist conditions by placing 30 drops of deionized water in different smoothed locations within the sampling area from a standard height of 10 mm and recording the time for their complete penetration. A medical dropper was used that yielded drops of uniform volume (70 ± 5 μl). According to Hallin, Douglas, Doerr, and Bryant (2013), the applied protocol allows estimating the mean WDPT value with an error of ±10% at 95% confidence. Five classes of repellency were considered: wettable (WDPT- 5 s), slightly water repellent (5 < WDPT ≤ 60 s); strongly water repellent (60 < WDPT ≤ 600 s); severely water repellent (600 < WDPT- 3,600 s), and extremely water repellent (WDPT > 3,600 s; Bisdom, Dekker, & Schoute, 1993; Dekker et al., 2009).

For each experimental condition, 5 to 10 infiltration tests were conducted by a standard MDI with a 45-mm-diameter disk and an imposed pressure head at the soil surface $h_0$ = −2 cm. Both 95% ethanol and deionized water were used, placing the disk of the MDI directly on the soil surface previously levelled using a spatula without adding or removing material from the infiltration spot. When necessary, soil depressions were filled by small amount of 2-mm sieved soil collected near the infiltration point. Infiltration spot preparation was therefore considered to not affect SWR estimation. A stand and a clamp were used to maintain the MDI upright. Approximately 50 mm of ethanol or water was allowed to infiltrate in each MDI test. Overall, 85 infiltration tests with ethanol and 85 infiltration tests with water were conducted at the experimental sites. Cumulative infiltration of ethanol was visually recorded at the MDI reservoir at intervals of 10 s for the first minute, every 30 s for the successive 2 min, and, finally, every 1 min until the complete infiltration of the prescribed volume (approximately 0.08 L, corresponding to a cumulative infiltration $I$ = 50 mm). Infiltration of water was much slower than infiltration of ethanol and, therefore, measurement intervals were increased up to 15 min. For 14 runs, the infiltration process was stopped before the MDI reservoir had completely emptied, but, in any case, test duration was at least 3 hr. Only for the 15 runs conducted with water at the fire-affected site of Javea, infiltration runs were stopped after 1.5 hr when average cumulative infiltration was 27.5 mm (0.044 L). This circumstance did not preclude application of Equation (2) to calculate $RI_s$. The depth of the wetting front, as detected by soil excavation at the end of the infiltration test, was generally limited to 4–5 cm.

Soil sorptivity using water, $S_w$, and ethanol, $S_e$, was estimated by different approaches: (a) $S = I_1/\sqrt{t}$, $I_1$ being the cumulative infiltration in the first minute of the run (one-minute approach, S1); (b) slope of the straight line describing the $I$ versus $\sqrt{t}$ relationship during the early stage of the infiltration process according to Philip (1957; short-time linearization[SL] approach); (c) intercept of the regression line fitting the linearized infiltration data in the form of $I/\sqrt{t}$ versus $\sqrt{t}$ (CL approach); and (d) intercept of the regression line fitting the linearized infiltration data in the form of $dI/d\sqrt{t}$ versus $\sqrt{t}$ (DL approach).

To exclude influence of soil spatial variability on RI estimation, the procedure proposed by Pekarova, Pekar, and Lichner (2015) was applied by considering all the possible combinations of estimated $S_e$ and $S_w$ values within an experimental site (i.e., 100 estimates of RI were obtained at the forest and grass sites of Ciavolo and Javea and 25 estimates at burned forest site of Javea). According to the different approaches, four RI datasets were obtained for each experimental condition (i.e., $RI_{S1}$, $RI_{SL}$, $RI_{CL}$, and $RI_{DL}$). For each MDI test conducted with water ($N$ = 85), a $RI_s$ value was calculated by Equation (2) using the linearized cumulative infiltration data in the form of CL ($RI_{s\text{-}CL}$) and DL ($RI_{s\text{-}DL}$) approaches.

According to the findings by Alagna et al. (2017), a log-normal distribution was considered for RI, $RI_s$, and WDPT, whereas a normal distribution was considered for other datasets (Coutinho et al., 2016; Di Prima et al., 2016). Mean and coefficient of variation (CV) of a given dataset were calculated according to the associated statistical distribution (Lee, Reynolds, Elrick, & Clothier, 1985). Comparisons between two mean values were conducted by a paired $t$ test, whereas comparisons among three mean values by a Tukey highly significant difference test. In both cases, a significance level of 0.05 was considered.

## 4 | RESULTS AND DISCUSSION

### 4.1 | MDI tests with ethanol

Cumulative infiltration of ethanol was in line with the infiltration theory given that a transient phase, in which infiltration rate decreased, was followed by a steady state infiltration phase in which infiltration rate was practically constant (Figure 2a). In most cases, the *I* versus *t* relationships appeared linear, with no concavity or a concavity limited to the very early stage of infiltration. This linear trend indicated that gravity and lateral capillary influenced the axisymmetric flow out of the disk source very soon after the beginning of the infiltration process (Bagarello, Ferraris, & Iovino, 2004; Di Prima et al., 2016; Dohnal et al., 2010; Vandervaere et al., 2000a, 2000b).

Steady state infiltration rate, $i_s$ (L/T), determined by the least-squares regression slope of the linear portion of the *I* versus *t* curve (Bagarello, Iovino, & Reynolds, 1999), ranged between 45.1 and 1,065 mm/hr (CV = 80.9%) and the minimum and maximum $i_s$ values were obtained for the organic soil at the pine forest sites of Javea (H-O-D) and Ciavolo (P-O-D), respectively, thus showing the large variability of conditions that may be encountered under a similar type of vegetation. The mean steady state infiltration rates were generally higher in the clay-loam soil of Ciavolo (P and G habitats) than in the sandy-loam and silt-clay soils of Javea (B and H habitats; Table 3).

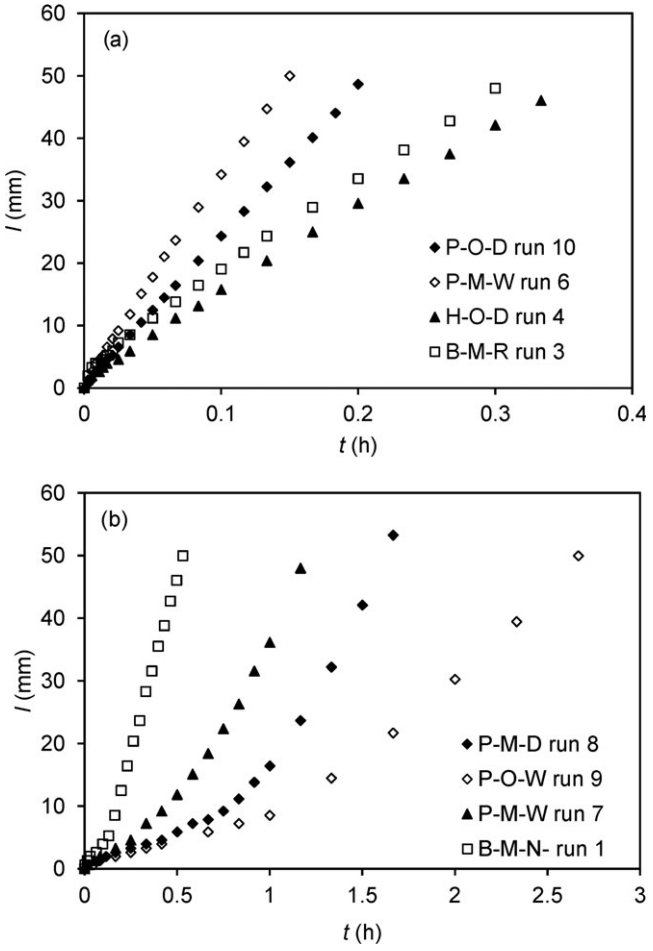


**FIGURE 2** Example of cumulative infiltration curves obtained in selected sites using (a) ethanol and (b) water as infiltrating fluid

**TABLE 3** Mean values of time to achieve steady state, $t_s$; steady state infiltration rate, $i_s$; and ethanol sorptivity, $S_e$, estimated according to different approaches from MDI tests conducted under different experimental conditions

| Experimental condition | *N* | $t_s$ (h) | $i_s$ (mm/hr) | Sorptivity, $S_e$ (mm/hr$^{0.5}$) | | | |
|---|---|---|---|---|---|---|---|
| | | | | S1 | SL | CL | DL |
| P-O-D | 10 | 0.021 | 624.1 | 104.4 | 79.9 | 34.8 | 38.1 |
| P-O-W | 10 | 0.051 | 402.4 | 33.0 | 26.9 | 9.5 | 8.0 |
| P-M-D | 10 | 0.119 | 219.2 | 51.4 | 44.3 | 13.6 | 15.5 |
| P-M-W | 10 | 0.055 | 293.1 | 48.4 | 36.1 | 13.7 | 17.3 |
| G-M-W | 10 | 0.102 | 175.4 | 33.0 | 33.8 | 15.4 | 12.2 |
| H-O-D | 10 | 0.137 | 107.2 | 25.5 | 23.6 | 14.2 | 11.5 |
| H-M-D | 10 | 0.108 | 100.7 | 27.8 | 24.0 | 16.9 | 16.2 |
| B-M-N | 5 | 0.103 | 106.7 | 33.0 | 27.2 | 20.4 | 24.9 |
| B-M-C | 5 | 0.120 | 122.8 | 41.2 | 36.6 | 29.1 | 28.9 |
| B-M-R | 5 | 0.087 | 166.6 | 46.1 | 41.6 | 29.2 | 30.1 |
| All data | N | 85 | 85 | 85 | 85 | 84 | 84 |
| | Min | 0.01 | 45.1 | 10.2 | 10.9 | 0.4 | 0.7 |
| | Max | 0.27 | 1065 | 163.0 | 128.4 | 61.7 | 68.4 |
| | Mean | 0.09 | 249.4 | 45.1a | 37.8b | 18.6c | 19.0c |
| | CV (%) | 72.1 | 80.9 | 67.5 | 60.4 | 71.3 | 74.2 |

*Note*. Mean values followed by the same letter are not statistically different according to a paired t-test ($P$ = 0.05). MDI, minidisk infiltrometer.

Limiting the analysis to the mineral soils (i.e., neglecting the organic soils for consistency among the three datasets collected at the different experimental sites), the steady state infiltration rates decreased in the order Ciavolo clay-loam (175–293 mm/hr, depending on the habitat) > Javea sandy-loam (107–167 mm/hr) > Javea silty-clay (101 mm/hr). Due to different surface tension and density of ethanol, the effective applied pressure head at the soil surface was −5 cm (Jarvis, Etana, & Stagnitti, 2008). As smaller conductive pores are more frequent in fine textured soils than in coarse textured porous media (e.g., Hillel, 1998), a higher value of $i_s$ in the clay-loam soil is not uncommon.

The time required to achieve steady state flow, $t_s$ (T) (Bagarello et al., 1999), was larger than the fixed time to estimate sorptivity according to the S1 approach ($t$ = 1 min) in 95.3% of cases. Therefore, obtaining steady-state flow required more than 1 min and thus a transient phase potentially usable to estimate sorptivity by both the S1 and SL approaches was available. As a matter of fact, plots of *I* versus $\sqrt{t}$ showed an initial linear part including at least four data points, thus allowing reliable estimates of soil sorptivity according to the SL approach. Mean values of ethanol sorptivity estimated according to the S1 and SL approaches for the different experimental conditions spanned over a similar range of values (Table 3) and the $S_e$ values estimated by the two approaches for each MDI test ($N$ = 85) were highly correlated (Figure 3a). However, a bias from the identity line was observed for high sorptivity values denoting that the influence of lateral capillary, and probably of gravity, comes into play even for time lower than 1 min. According to a paired $t$ test ($P$ = 0.05), the two approaches were not equivalent in estimating $S_e$ (Table 3).

A linear relationship between $I/\sqrt{t}$ and $\sqrt{t}$ (CL approach) and between $dI/d\sqrt{t}$ and $\sqrt{t}$ (DL approach) was visually recognized for

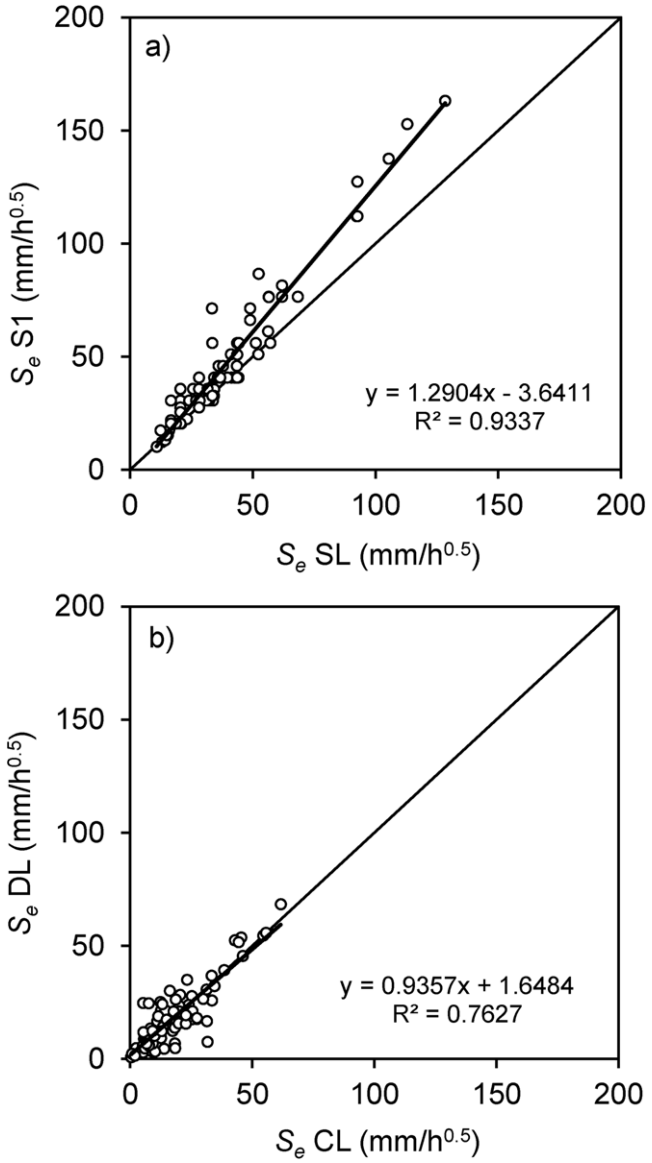


**FIGURE 3** Comparison between ethanol sorptivity values, Se, estimated according to different approaches: (a) short-time linearization (SL) versus S1; (b) cumulative linearization (CL) versus differentiated linearization (DL)

the entire duration of the infiltration test in most cases (77% and 79%, respectively). In the remaining cases, a definite linear trend including at least 50% of the cumulative infiltration data was detected, thus suggesting that both approaches were always applicable. Applicability of Equation 1 was statistically assessed by calculating the coefficients of determination, $R^2$, for the $I/\sqrt{t}$ versus $\sqrt{t}$ and $dI/d\sqrt{t}$ versus $\sqrt{t}$ linear regressions. In particular, $R^2$ values for each infiltration test were always significant ($P$ = 0.05) and higher than 0.629 for the CL approach (mean $R^2$ = 0.977) and 0.513 (mean $R^2$ = 0.859) for the DL approach. Mean $S_e$ values estimated by the CL and DL approaches were not significantly different (Table 3), and the regression line between the single $S_e$ estimates obtained by the two approaches ($N$ = 84) was not different from the identity line (Figure 3b). However, mean $S_e$ values obtained by the experimental information collected from early to intermediate infiltration time (CL and DL approaches) were lower than those obtained using only the early-time information (Table 3). Therefore, the four considered approaches for estimating ethanol sorptivity were not equivalent and a systematic overestimation of $S_e$ was observed for the approaches (S1 and SL) that make use of early-time infiltration data only. This result makes the choice to calculate $S_e$ using only infiltration data collected in the early stage of the infiltration process questionable.

## 4.2 | MDI tests with water

Plots of cumulative water infiltration versus time typically exhibited an upward convex shape that is indicative of water repellency occurrence (Figure 2b). In particular, the increase in infiltration rates with time suggests a reduction in SWR as infiltration proceeds (Beatty & Smith, 2013; Carrick et al., 2011; Di Prima et al., 2016; Ebel & Moody, 2013; Imeson et al., 1992). Prolonged contact with water can lead to the loss of SWR as a consequence of the changes in orientation of amphiphilic molecules on a mineral surface while in contact with water (Doerr et al., 2000). The WDPT test (Van't Woudt, 1959), for example, is a measure of the duration of this process which depends on a variety of biotic and abiotic factors and leads to a wettable soil and, thus, to an increase in infiltration rate.

Due to hydrophobicity, the time needed for total water volume to infiltrate ($I$ = 50 mm) was much longer than with ethanol ranging up to 9 hr (Table 4). Mean values of the infiltration rate $\bar{i}$, that is, the ratio between the final cumulative volume and the corresponding duration, were lower for the organic soils ($3.8 \leq \bar{i} \leq 12.6$ mm/hr) than mineral soils ($17.5 \leq \bar{i} \leq 126.6$ mm/hr; Table 4). The highest $\bar{i}$ values were obtained in the glade site of Ciavolo (G-M-W; $\bar{i}$ = 101.7 mm/hr) and in the mineral subsoil of the pine forest in Javea (H-M-D; $\bar{i}$ = 126.6 mm/hr).

**TABLE 4** Mean values of duration, $t_{tot}$; infiltration rate, $\bar{i}$; and water sorptivity, $S_w$, estimated according to different approaches from MDI tests conducted under different experimental conditions

| Experimental condition | $N$ | $t_{tot}$ (hr) | $\bar{i}$ (mm/hr) | Sorptivity, $S_w$ (mm/hr$^{0.5}$) | | | |
|---|---|---|---|---|---|---|---|
| | | | | S1 | SL | CL | DL |
| P-O-D | 10 | 7.10 | 7.0 | 5.4 | 2.7 | 1.7 | 1.5 |
| P-O-W | 10 | 4.18 | 12.6 | 6.9 | 8.1 | 4.9 | 3.5 |
| P-M-D | 10 | 2.47 | 24.8 | 6.8 | 3.1 | 1.6 | 1.1 |
| P-M-W | 10 | 2.14 | 26.8 | 7.9 | 7.1 | 6.2 | 5.4 |
| G-M-W | 10 | 0.53 | 101.7 | 22.9 | 24.1 | 14.9 | 12.8 |
| H-O-D | 10 | 4.34 | 3.8 | n.a. | 2.0 | 0.8 | 1.3 |
| H-M-D | 10 | 0.41 | 126.6 | 42.8 | 37.9 | 33.7 | 33.0 |
| B-M-N | 5 | 0.86 | 44.4 | 10.0 | 9.0 | 6.6 | 4.2 |
| B-M-C | 5 | 1.38 | 17.5 | 9.4 | 9.0 | 6.8 | 5.8 |
| B-M-R | 5 | 1.78 | 19.0 | 5.1 | 6.9 | 5.2 | 5.7 |
| All data | N | 85 | 85 | 49 | 85 | 80 | 82 |
| | Min | 0.2 | 0.7 | 5.1 | 0.9 | 0.2 | 0.2 |
| | Max | 9.0 | 249.9 | 76.4 | 63.9 | 60.1 | 61.5 |
| | Mean | 2.7 | 40.4 | 18.0a | 11.5b | 9.0b | 8.0b |
| | CV (%) | 86.1 | 125.0 | 93.8 | 115.6 | 133.1 | 147.3 |

*Note*. Mean values followed by the same letter are not statistically different according to a paired $t$ test ($P$ = 0.05). MDI, minidisk infiltrometer.

The very slow infiltration in the early stages of the process made the estimation of soil water sorptivity, $S_w$, problematic. Indeed, in 36 infiltration tests conducted with water (42% of cases), water flow out of the MDI did not start during the first minute of infiltration, making it impossible to estimate $S_w$ by the S1 approach. Wetting of soil surface, as detected by the rising of the first air bubble within the MDI reservoir, was particularly slow in the organic soil of the pinus forests (P-O-D, P-O-W, and H-O-D), where the average time for the start of infiltration was 705 s (maximum value = 3,000 s). For the remaining 49 runs, the $S_w$ values calculated by the S1 approach ranged from 5.1 to 76.4 mm/hr$^{0.5}$, with a mean value of 18.0 mm/hr$^{0.5}$ (CV = 93.8%). According to a paired $t$ test ($P$ = 0.05), mean $S_w$ estimated from the same experimental dataset by the S1 approach was higher than the sorptivity estimated by the remaining three approaches (SL, CL, and DL; Table 4).

Despite the difficulties in detecting the start of the wetting process, analysis of water infiltration data confirmed the results obtained with ethanol as infiltrating fluid. A criterion based on a fixed short time (1 min in this case) tended to overestimate both ethanol and water sorptivity, whereas in extremely water repellent soils, it was not appropriate for assessing the initial stage of infiltration. Therefore, its application as a general criterion for assessing repellency is questionable. Maybe, the poor applicability of S1 approach in strongly hydrophobic soils could be overcome by selecting a shorter time interval for ethanol infiltration and a larger time interval for water infiltration but this choice appears arbitrary and would probably hinder the benefit of rapidity and simplicity for which this approach has been proposed (Lewis et al., 2006; Robichaud et al., 2008). Due to this drawback, the S1 approach was excluded from the subsequent analysis on the assessment of SWR.

The CL and DL approaches could not be applied in five and three cases out of 85, respectively, as it was not possible to identify a monotonic increasing trend in the $I/\sqrt{t}$ versus $\sqrt{t}$ or $dI/d\sqrt{t}$ versus $\sqrt{t}$ data or the intercept of the regression line was negative. The SL, CL, and DL approaches yielded statistically equivalent estimates of $S_w$ (Table 4) even if an overestimation of sorptivity was detected when only early-time infiltration data were used (SL approach; Figure 4). For water infiltration tests, gravity and lateral capillary probably came into play at a later stage of the infiltration process as compared with the ethanol infiltration tests and, therefore, the SL approach did not result in $S_w$ overestimation similar to those detected, by the same approach, for $S_e$. The $S_w$ values estimated by the linearization approaches (i.e., CL and DL) were not significantly different (Table 4), and the linear regression line between the individual $S_w$ estimates was not different from the identity line (confidence intervals for intercept and slope: −1.29–0.22, 0.91–1.01, respectively; Figure 4).

## 4.3 | Classical repellency index

Independently of the estimation approach (SL, CL, or DL), mean $S_e$ values for each experimental condition (Table 3) were higher than the corresponding $S_w$ values (Table 4), the only exception being for the mineral soil of the pine forest of Javea (H-M-D) in which nonrepellent conditions were clearly observed during field tests.

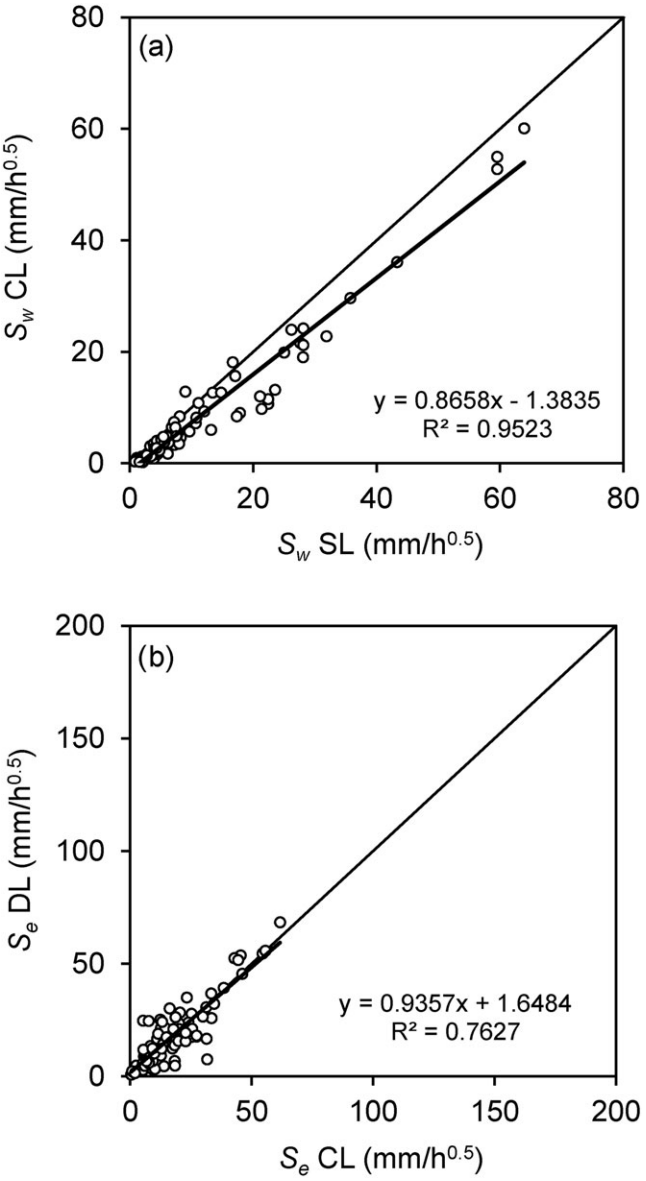


**FIGURE 4** Comparison between water sorptivity values, $S_w$, estimated according to different approaches: (a) short-time linearization (SL) versus cumulative linearization (CL); (b) CL versus differentiated linearization (DL)

Estimation of the repellency index according to the classical procedure by Tillman et al. (1989) depended on the approach followed to estimate $S_e$ and $S_w$ (Table 5). According to a Tukey highly significant difference test, discrepancies between the RI values calculated with different sorptivity estimation approaches (i.e., $RI_{SL}$, $RI_{CL}$, and $RI_{DL}$) tended to be less pronounced in hydrophobic soils than in less water repellent soils. Depending on the experimental condition, the ratio $RI_{SL}/RI_{CL}$ ranged between 0.93 and 3.24, whereas $RI_{SL}/RI_{DL}$ was in the range 0.51–2.11. On average, $RI_{SL}$ overestimated SWR, as compared with $RI_{CL}$ and $RI_{DL}$ by a factor of 1.57 and 1.23, respectively (Table 5). In 8 out of 10 experimental conditions, $RI_{CL}$ and $RI_{DL}$ were not statistically different. This was an expected result given that the $S_e$ and $S_w$ values estimated by the two approaches were not statistically different (Tables 3 and 4) and the scatterplots of $S_e$ and $S_w$ were close to the 1:1 line (Figures 3b and 4b). In 70% of the cases, $RI_{SL}$ differed from those calculated by one or both alternative approaches

**TABLE 5** Mean values of RI (Tillman et al., 1989) calculated according to SL, CL, and DL approaches for the experimental conditions considered

| Experimental condition | $RI_{SL}$ | $RI_{CL}$ | $RI_{DL}$ |
|---|---|---|---|
| P-O-D | 55.1a | 45.4a | 52.3a |
| P-O-W | 32.5a | 19.5b | 28.5ab |
| P-M-D | 6.1a | 1.9b | 3.6a |
| P-M-W | 9.7a | 3.6b | 4.6b |
| G-M-W | 2.7a | 2.0b | 1.7b |
| H-O-D | 22.4a | 18.9a | 19.3a |
| H-M-D | 1.3a | 1.0b | 1.0b |
| B-M-N | 6.6a | 6.6a | 12.8b |
| B-M-C | 8.0a | 8.3ab | 10.5b |
| B-M-R | 11.1a | 10.4a | 10.5a |

Mean values on a row followed by the same letter are not statistically different according to highly significant difference (HSD) Tukey test ($P$ = 0.05). CL, cumulative linearization; DL, differentiated linearization; RI, repellency index; SL, short-time linearization.

and most of the differences occurred because the SL approach yielded higher SWR estimation than the CL and/or DL approaches. Therefore, the SL approach for estimating ethanol and water sorptivities may result in RI overestimation, particularly under low SWR conditions.

The two approaches based on the linearization of the cumulative infiltration curve yielded generally similar estimates of RI and can therefore be considered equally usable for field estimation of SWR. Moreover, these estimates of RI could be expected to be reliable because they are based on an approach that distinguishes among the different forces driving infiltration. However, a negative aspect of using linearization approaches is that $S$ estimation may be affected by a subjective selection of the linear part of the $I/\sqrt{t}$ versus $\sqrt{t}$ and $dI/d\sqrt{t}$ versus $\sqrt{t}$ plots to be used for fitting Equation 1 to the data (Bagarello & Iovino, 2004; Vandervaere et al., 2000a, 2000b). In general, selection of data describing a linearly increasing relationship was easier on the CL than the DL plot due to the scattering effect associated to the finite difference calculation of the term $dI/d\sqrt{t}$ (Figure 5).

The RI value for H-M-D was lower than 1.95 (Table 5), which was considered by Tillman et al. (1989) as the value discriminating between nonrepellent and repellent conditions. It is worth noting that the RI values were always higher in the surface organic horizons than in the underlying mineral ones with values ranging up to RI = 55 under dry conditions. However, relatively high RI values were also observed in the mineral horizon of the pine forest of Ciavolo (P-M-D and P-M-W) and also in the burned site of Javea mulched with chopped pine residues (B-M-R; Table 5). As highlighted by Alagna et al. (2017), leaching of hydrophobic compound from the overlying organic duff or mulching layer could be responsible for these findings.

## 4.4 | New repellency index

The total cumulative water infiltration data, linearized in the form of either CL or DL approaches, always showed an increasing trend that was characterized by a practically unique slope in nonrepellent soils (Figure 5b,d) and, conversely, showed a typical *hockey-stick-like* shape in water repellent soils (Figure 5a,c). In the latter case, the experimental plot was characterized by an initial increasing linear part followed, after a knee, by a more or less pronounced increase in slope. Independently of the shape of the linearized plot, the slopes for the initial and

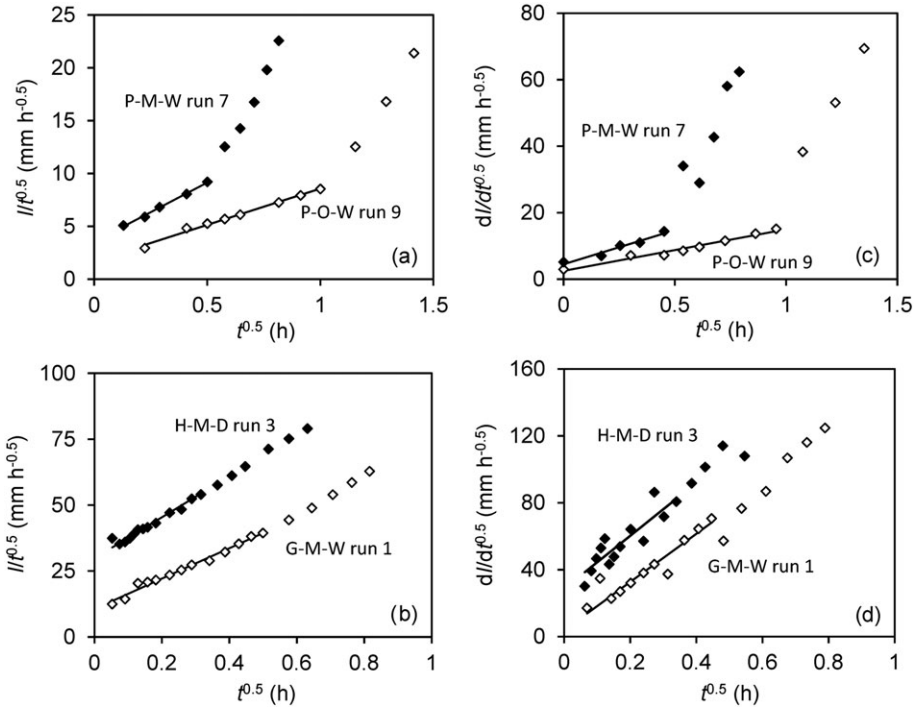


**FIGURE 5** Examples of application of cumulative linearization approach (a and b) and differentiated linearization differentiated linearization approach (c and d) to water infiltration experiments in hydrophobic (a and c) and nonhydrophobic (b and d) soils

the later stages of the infiltration processes were calculated. Identification was easy in 94% of the cases for the CL approach and in 80% of the cases when the DL approach was considered. In one case only, the two approaches were not applicable. In the remaining cases (i.e., 6% of cases for CL and 20% for DL), the estimation of one of the two slopes was characterized by a very small number of points (i.e., three points), or a low, nonsignificant coefficient of correlation was found. Nevertheless, a meaningful trend was always visually detectable and, therefore, these estimations were maintained in the dataset.

The mean $RI_s$ values calculated by the CL and DL approaches were not statistically different in 8 out of 10 experimental conditions (Table 6), and the regression line between the $RI_{s\text{-}CL}$ and $RI_{s\text{-}DL}$ was characterized by a significant $R^2$ = 0.9663 and was not different from the identity line (confidence intervals for intercept and slope: −1.26–3.17, 0.87–1.18, respectively). Depending on the considered experimental condition, the $RI_{s\text{-}CL}$ values ranged from 1.2 to 37.9 and the $RI_{s\text{-}DL}$ from 1.7 to 39.3 (Table 6). The clear increasing trend of $RI_s$ at increasing soil hydrophobicity was confirmed by the significant correlations that were found, independently of the approach (CL or DL), with the classical RI and WDPT indices (Table 7). In particular, the new $RI_s$ index detected repellency condition for the mineral soil of the glade at Ciavolo (G-M-W; $RI_s$ = 2.3–2.7) that was classified as not repellent according to the traditional WDPT test (mean WDPT < 5 s). This result was in line with RI values that ranged between 1.7 and 2.7 (Table 5), thus confirming that the $RI_s$ index can be able to detect slight SWR conditions that could be not assessed by the commonly used WDPT classification (Bisdom et al., 1993; Dekker et al., 2009). On the other hand, inconsistency between WDPT and RI or $RI_s$ was observed for the organic layer of Javea forest site (H-O-D) that was severely water repellent according to the WDPT test ($t$ = 2139 s) but slightly water repellent according to the RI and $RI_s$ tests (Figure 6). As a consequence of this discrepancy, the coefficients of determination for $RI_{s\text{-}CL}$ versus WDPT and $RI_{s\text{-}DL}$ versus WDPT linear regressions were low despite still significant ($P$ = 0.05; Table 7). When the point corresponding to this experimental condition was excluded from the regression analysis, the coefficient of determination increased up to $R^2$ = 0.8803 ($P$ = 0.01) for $RI_{s\text{-}CL}$ versus WDPT

**TABLE 7** Coefficients of determination for linear regressions between the repellency index, $RI_s$ (Equation (2)); calculated according to both the CL and DL approaches and the repellency index, RI; and the water drop penetration time (WDPT) for the experimental conditions considered ($N$ = 10)

| Linear regression | $R^2$ | $P$ |
|---|---|---|
| $RI_s$ CL vs. RI CL | 0.753 | ** |
| $RI_s$ CL vs. RI DL | 0.805 | ** |
| $RI_s$ CL vs. WDPT | 0.378 | * |
| $RI_s$ DL vs. RI CL | 0.730 | ** |
| $RI_s$ DL vs. RI DL | 0.763 | ** |
| $RI_s$ DL vs. WDPT | 0.459 | * |

*Significant at $P$ = 0.05.

**Significant at $P$ = 0.01.

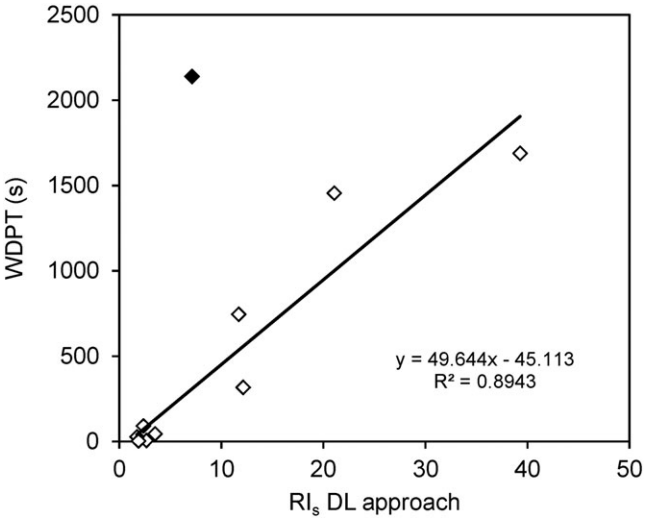


**FIGURE 6** Relationship between the repellency index $RI_s$ calculated by the differentiated linearization (DL) approach and the water drop penetration time (WDPT) for the different experimental conditions considered ($N$ = 9). The filled dot refers to the data collected in the organic layer of Javea forest site (H-O-D) that was excluded from the regression analysis

**TABLE 6** Statistics of the new repellency index $RI_s$ (Equation (2)) calculated according to CL and DL approaches for the experimental conditions considered

| Experimental condition | $RI_{s\text{-}CL}$ | | | | | $RI_{s\text{-}DL}$ | | | | |
|---|---|---|---|---|---|---|---|---|---|---|
| | $N$ | min | max | Geometric mean | CV (%) | $N$ | min | max | Geometric mean | CV (%) |
| P-O-D | 10 | 1.8 | 107.8 | 37.9a | 92.4 | 10 | 1.3 | 99.1 | 39.3a | 80.9 |
| P-O-W | 10 | 5.5 | 47.3 | 18.9a | 63.9 | 10 | 2.7 | 59.6 | 21.1a | 96.1 |
| P-M-D | 10 | 2.9 | 11.4 | 7.1a | 38.6 | 10 | 3.9 | 27.4 | 12.1b | 55.1 |
| P-M-W | 10 | 2.9 | 24.3 | 10.2a | 64.7 | 10 | 3.7 | 22.4 | 11.7a | 61.7 |
| G-M-W | 10 | 1.3 | 3.2 | 2.3a | 22.4 | 10 | 1.4 | 4.0 | 2.7a | 27.4 |
| H-O-D | 10 | 2.0 | 10.3 | 3.6a | 68.8 | 10 | 0.7 | 8.5 | 4.0a | 59.9 |
| H-M-D | 10 | 1.1 | 5.2 | 2.4a | 61.6 | 10 | 0.9 | 3.1 | 1.9a | 37.9 |
| B-M-N | 4 | 1.2 | 11.8 | 5.7a | 91.5 | 4 | 1.5 | 4.5 | 2.4a | 59.9 |
| B-M-C | 5 | 1.4 | 3.0 | 1.8a | 38.2 | 5 | 1.4 | 7.8 | 3.5a | 75.1 |
| B-M-R | 5 | 1.0 | 1.4 | 1.2a | 12.8 | 5 | 1.0 | 2.0 | 1.7b | 24.6 |

*Note*. For a given experimental condition, mean values followed by the same letter are not statistically different according to a paired $t$ test ($P$ = 0.05). CL, cumulative linearization; CV, coefficient of variation; DL, differentiated linearization.

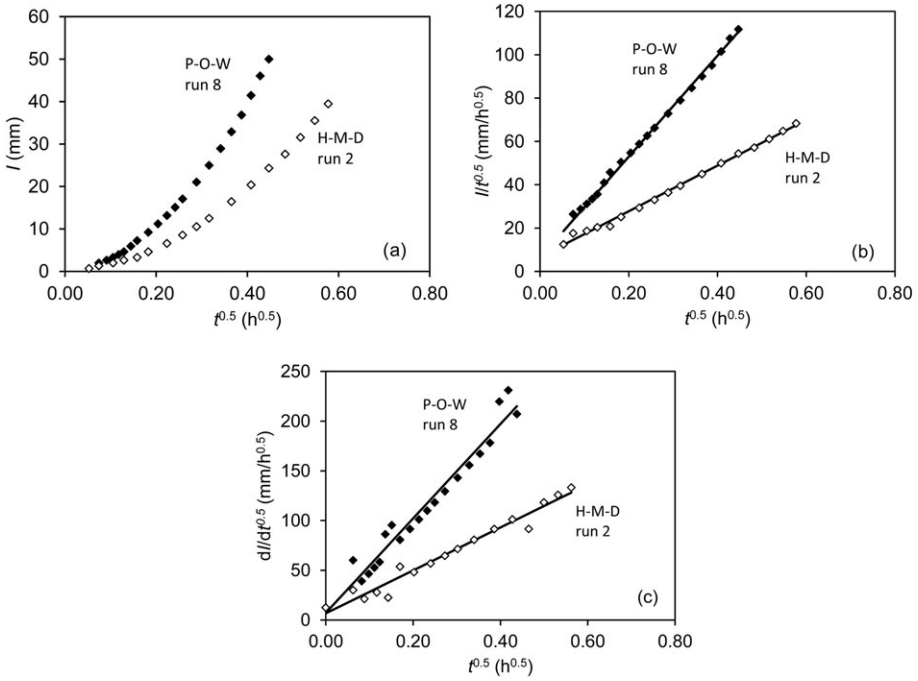


**FIGURE 7** Examples of cumulative ethanol infiltration curves plotted according to different representations: (a) linearization of the early-time infiltration data in the form I versus t0.5, (b) linearization of the complete infiltration curve according to cumulative linearization approach, and (c) linearization of the complete infiltration curve according to differentiated linearization approach

linear regression and $R^2$ = 0.8943 ($P$ = 0.01) for $RI_{s\text{-}DL}$ versus WDPT one. Despite WDPT and $RI_s$ explore different soil volumes and, thus, are probably not fully comparable, testing the new proposed $RI_s$ with available and well-assessed technique, like WDPT, is the only viable approach to assess its reliability. Comparisons between infiltration based repellency indices and WDPT were conducted, among others, by Bughici and Wallach (2016), Lewis et al. (2006), and Schacht, Chen, Tarchitzky, Lichner, and Marschner (2014). The significant correlation found under different soil/vegetation/management conditions is encouraging and supports the conclusion that the information gathered from a single water infiltration experiment conducted by the MDI for a relatively long time interval is potentially exploitable to assess SWR.

Similar conclusions were drawn by Lichner et al. (2013), who proposed to assess the soil hydrophobicity by the WRCT that was estimated as the intersection between the two regression lines representing the early-time (hydrophobic) and late-time (wettable) conditions when the cumulative infiltration data are plotted on a $I$ versus $\sqrt{t}$ plot. The new proposed $RI_s$ was significantly correlated with WRCT calculated according to Lichner et al. (2013; $R^2$ = 0.8385 for $RI_{s\text{-}CL}$ versus WRCT linear regression and $R^2$ = 0.8466 for $RI_{s\text{-}DL}$ versus WRCT one). For the reduced dataset collected only at the forested sites of Ciavolo and Javea, Alagna et al. (2017) also tested a modified repellency index, $RI_m$, defined as the ratio of the slopes of the $I$ versus $\sqrt{t}$ plot at the late and early stages of the infiltration process (Sepehrnia, Hajabbasi, Afyuni, & Lichner, 2016). However, both the WRCT and the $RI_m$ are obtained from the $I$ versus $\sqrt{t}$ plot of cumulative water infiltration data. The new repellency index $RI_s$ seems to be more physically robust than WRCT and $RI_m$ indices as these two approaches neglect the influence of gravity and lateral capillary that comes into play after the very early-time stage of the infiltration process. Actually, plots of $I$ versus $\sqrt{t}$ may exhibit an upward convex shape that is not due to increased soil wettability as infiltration proceeds but depends on the progressively increasing importance of gravity and lateral capillary flow (Cook & Broeren, 1994; Smettem, Ross, Haverkamp, & Parlange, 1995). Using cumulative infiltration data in the form of $I$ versus $\sqrt{t}$ plot may thus misestimate the repellency phenomena. In Figure 7, for two ethanol tests, infiltration data are plotted in $I$ versus $\sqrt{t}$ form and according to CL and DL linearization approaches. As can be seen, CL and DL plots (Figure 7b,c) are clearly linear, as they should be for ethanol infiltration, whereas $I$ versus $\sqrt{t}$ plot shows an increasing slope that might be attributed to an artefact water repellency that is not real in fact. On the other hand, the repellency index calculated according to Equation (2) includes information on both sorptivity and conductivity measured in the wettable and repellent stages of the infiltration process and, therefore, it can be considered more directly linked to the hydrological processes affected by SWR.

## 5 | CONCLUSIONS

The adjusted ratio between ethanol and water sorptivities, estimated by a tension infiltration experiment, is a valuable tool to assess the extent of SWR. However, the commonly applied horizontal infiltration equation that makes use only of the initial stage of the axisymmetric flow out of a MDI may result in overestimations of sorptivity due to the neglected effects of gravity and lateral capillary on infiltration. The two-term infiltration model proposed by Haverkamp et al. (1994), that is valid for early to intermediate infiltration times, is potentially more able to yield unbiased estimations of sorptivity. For

variable experimental conditions resulting from different soil texture, vegetation habitat, sampled horizon, soil management, and initial water content, the approaches based on the linearization of the two-term infiltration model (CL and DL) yielded similar estimates of $S_e$ and $S_w$. A systematic overestimation of $S_e$ was observed with approaches (S1 and SL) that make use of early-time infiltration data only. Moreover, the S1 approach was inapplicable in 42% of experiments conducted with water, thus preventing estimation of the repellency index, RI, proposed by Tillman et al. (1989). The biases in $S_e$ and $S_w$ estimations obtained by the SL approach yielded an overestimation of RI by a factor of 1.57 and 1.23 as compared with the values estimated with the CL and DL approaches. Moreover, these discrepancies were more pronounced in less water repellent soils.

For the experimental conditions considered, the mean values of the new repellency index, the $RI_s$, defined as the ratio of the slopes of the linearized cumulative infiltration data in the wettable and repellent stages of infiltration, were significantly correlated with the mean RI and WDPT indices, thus showing the potential reliability of soil hydrophobicity assessment by this index. Compared with the RI index, $RI_s$ is estimated from a single water infiltration experiment conducted by the MDI, as well as other tension infiltrometers, thus overcoming drawbacks of conducting paired water and ethanol infiltration experiments in two different spots (i.e., small-scale spatial variability and variable temperature effect on the physical characteristics of the two infiltrating liquids). As for previously proposed repellency indices (i.e., WRCT and $RI_m$), the new $RI_s$ offers a way to quantify with a single number the complex site-specific soil wetting properties. However, $RI_s$ appears physically more sound in that it includes information on both sorptivity and hydraulic conductivity measured in the early repellent and subsequent wettable stages of the infiltration process thus being more directly linked to the hydrological processes affected by SWR.

Further investigations are necessary to test the validity of the new index on different SWR conditions also with the aim to define classification criteria more quantitatively associated to the actual water-solid contact angle.

## ACKNOWLEDGMENTS

This study was supported by grants from the Università degli Studi di Palermo (Dottorato di Ricerca in Scienze Agrarie, Forestali e Ambientali, ciclo XXIX, D50002D13+1012), Ministero dell'Istruzione, dell'Università e della Ricerca (PRIN 2015 project GREEN4WATER B72F16000550005), the Slovak Research and Development Agency APVV (project APVV-15-0160), Ministerio de Economía and Competitividad of Spanish Government (project CGL2013-47862-C2-1-R), Botánica Mediterránea S.L., and Montgó Natural Park. Field data in Italy and Spain were collected by V. Alagna. All authors analysed the data and contributed to write the manuscript.

## ORCID

*Vincenzo Alagna* https://orcid.org/0000-0002-0936-2652
*Massimo Iovino* https://orcid.org/0000-0002-3454-2030
*Vincenzo Bagarello* https://orcid.org/0000-0003-3575-549X
*Jorge Mataix-Solera* https://orcid.org/0000-0003-2789-9936
*Lubomir Lichner* https://orcid.org/0000-0001-6057-1903

## REFERENCES

Alagna, V., Bagarello, V., Di Prima, S., & Iovino, M. (2016). Determining hydraulic properties of a loam soil by alternative infiltrometer techniques. *Hydrological Processes*, *30*(2), 263–275. https://doi.org/10.1002/hyp.10607

Alagna, V., Iovino, M., Bagarello, V., Mataix-Solera, J., & Lichner, L. (2017). Application of minidisk infiltrometer to estimate water repellency in Mediterranean pine forest soils. *Journal of Hydrology and Hydromechanics*, *65*(3), 254–263. https://doi.org/10.1515/johh-2017-0009

Angulo-Jaramillo, R., Bagarello, V., Iovino, M., & Lassabatere, L. (2016). Unsaturated soil hydraulic properties. In *Infiltration measurements for soil hydraulic characterization* (pp. 181–287). Cham: Springer International Publishing. https://doi.org/10.1007/978-3-319-31788-5_3

Bagarello, V., Di Prima, S., Iovino, M., & Provenzano, G. (2014). Estimating field-saturated soil hydraulic conductivity by a simplified Beerkan infiltration experiment. *Hydrological Processes*, *28*(3), 1095–1103. https://doi.org/10.1002/hyp.9649

Bagarello, V., Ferraris, S., & Iovino, M. (2004). An evaluation of the single-test tension infiltrometer method for determining the hydraulic conductivity of lateral capillarity domain Soils. *Biosystems Engineering*, *87*(2), 247–255. https://doi.org/10.1016/j.biosystemseng.2003.11.007

Bagarello, V., & Iovino, M. (2003). Field testing parameter sensitivity of the two-term infiltration equation using differentiated linearization. *Vadose Zone Journal*, *2*(3), 358–367. https://doi.org/10.2136/vzj2003.3580

Bagarello, V., & Iovino, M. (2004). Indagine di laboratorio su una metodologia innovativa per la determinazione della conducibilità idraulica del suolo con l'infiltrometro a depressione. *Rivista di Ingegneria Agraria*, *35*(2), 81–92.

Bagarello, V., Iovino, M., & Reynolds, W. D. (1999). Measuring hydraulic conductivity in a cracking clay soil using the Guelph Permeameter. *Transactions of the ASAE*, *42*(4), 957–964. https://doi.org/10.13031/2013.13276

Beatty, S. M., & Smith, J. E. (2013). Dynamic soil water repellency and infiltration in post-wildfire soils. *Geoderma*, *192*, 160–172. https://doi.org/10.1016/j.geoderma.2012.08.012

Bisdom, E. B. A., Dekker, L. W., & Schoute, J. F. T. (1993). Water repellency of sieve fractions from sandy soils and relationships with organic material and soil structure. *Geoderma*, *56*(1), 105–118. https://doi.org/10.1016/0016-7061(93)90103-R

Bughici, T., & Wallach, R. (2016). Formation of soil–water repellency in olive orchards and its influence on infiltration pattern. *Geoderma*, *262*, 1–11. https://doi.org/10.1016/j.geoderma2015.08.002

Carrick, S., Buchan, G., Almond, P., & Smith, N. (2011). Atypical early-time infiltration into a structured soil near field capacity: The dynamic interplay between sorptivity, hydrophobicity, and air encapsulation. *Geoderma*, *160*(3–4), 579–589. https://doi.org/10.1016/j.geoderma.2010.11.006

Carrillo, M. L. K., Yates, S. R., & Letey, J. (1999). Measurement of initial soil-water contact angle of water repellent soils. *Soil Science Society of America Journal*, *63*(3), 433–436. https://doi.org/10.2136/sssaj1999.03615995006300030002x

Cerdà, A., & Doerr, S. H. (2007). Soil wettability, runoff and erodibility of major dry-Mediterranean land use types on calcareous soils. *Hydrological Processes*, *21*(17), 2325–2336. https://doi.org/10.1002/hyp.6755

Cook, F. J., & Broeren, A. (1994). Six methods for determining sorptivity and hydraulic conductivity with disk permeameters. *Soil Science*, *157*(1), 2–11. https://doi.org/10.1097/00010694-199401000-00002

Coutinho, A. P., Lassabatere, L., Montenegro, S., Antonino, A. C. D., Angulo-Jaramillo, R., & Cabral, J. J. S. P. (2016). Hydraulic characterization and hydrological behaviour of a pilot permeable pavement in an urban centre, Brazil. *Hydrological Processes*, *30*(23), 4242–4254. https://doi.org/10.1002/hyp.10985

DeBano, L. F. (2000). Water repellency in soils: A historical overview. *Journal of Hydrology*, *231–232*(0), 4–32. https://doi.org/10.1016/S0022-1694(00)00180-3

Dekker, L. W., Doerr, S. H., Oostindie, K., Ziogas, A. K., & Ritsema, C. J. (2001). Water repellency and critical soil water content in a dune sand. *Soil Science Society of America Journal*, *65*(6), 1667–1674. https://doi.org/10.2136/sssaj2001.1667

Dekker, L. W., Oostindie, K., & Ritsema, C. J. (2005). Exponential increase of publications related to soil water repellency. *Australian Journal of Soil Research*, *43*(3), 403–441. https://doi.org/10.1071/SR05007

Dekker, L. W., Ritsema, C. J., Oostindie, K., Moore, D., & Wesseling, J. G. (2009). Methods for determining soil water repellency on field-moist samples. *Water Resources Research*, *45*. https://doi.org/10.1029/2008wr007070 Artn W00d33

Di Prima, S., Lassabatere, L., Bagarello, V., Iovino, M., & Angulo-Jaramillo, R. (2016). Testing a new automated single ring infiltrometer for Beerkan infiltration experiments. *Geoderma*, *262*, 20–34. https://doi.org/10.1016/j.geoderma.2015.08.006

Doerr, S. H. (1998). On standardizing the 'Water Drop Penetration Time' and the 'Molarity of an Ethanol Droplet' techniques to classify soil hydrophobicity: A case study using medium textured soils. *Earth Surface Processes and Landforms*, *23*(7), 663–668. https://doi.org/10.1002/(SICI)1096-9837(199807)23:7<663::AID-ESP909>3.0.CO;2-6

Doerr, S. H., Shakesby, R. A., & Walsh, R. P. D. (2000). Soil water repellency: its causes, characteristics and hydro-geomorphological significance. *Earth-Science Reviews*, *51*(1–4), 33–65. https://doi.org/10.1016/S0012-8252(00)00011-8

Dohnal, M., Dusek, J., & Vogel, T. (2010). Improving hydraulic conductivity estimates from minidisk infiltrometer measurements for soils with wide pore-size distributions. *Soil Science Society of America Journal*, *74*(3), 804. https://doi.org/10.2136/sssaj2009.0099

Ebel, B. A., & Moody, J. A. (2013). Rethinking infiltration in wildfire-affected soils. *Hydrological Processes*, *27*(10), 1510–1514. https://doi.org/10.1002/hyp.9696

Ebel, B. A., Moody, J. A., & Martin, D. A. (2012). Hydrologic conditions controlling runoff generation immediately after wildfire. *Water Resources Research*, *48*. https://doi.org/10.1029/2011wr011470. Artn W03529

Gee, G. W., & Bauder, J. W. (1986). Particle-size analysis. In A. Klute (Ed.), *Methods of soil analysis, part 1: Physical and mineralogical methods* (2nd ed.) (pp. 383–411). Madison, WI: ASA- SSSA.

Gonzalez-Sosa, E., Braud, I., Dehotin, J., Lassabatere, L., Angulo-Jaramillo, R., Lagouy, M., … Michel, K. (2010). Impact of land use on the hydraulic properties of the topsoil in a small French catchment. *Hydrological Processes*, *24*(17), 2382–2399. https://doi.org/10.1002/Hyp.7640

Hallett, P. D., & Young, I. M. (1999). Changes to water repellence of soil aggregates caused by substrate-induced microbial activity. *European Journal of Soil Science*, *50*(1), 35–40. https://doi.org/10.1046/j.1365-2389.1999.00214.x

Hallin, I., Douglas, P., Doerr, S. H., & Bryant, R. (2013). The role of drop volume and number on soil water repellency determination. *Soil Science Society of America Journal*, *77*(5), 1732–1743. https://doi.org/10.2136/sssaj2013.04.0130

Haverkamp, R., Ross, P. J., Smettem, K. R. J., & Parlange, J. Y. (1994). 3-dimensional analysis of infiltration from the disc infiltrometer. 2. Physically-based infiltration equation. *Water Resources Research*, *30*(11), 2931–2935. https://doi.org/10.1029/94wr01788

Hillel, D. (1998). *Environmental soil physics*. San Diego, CA: Academic Press.

Hunter, A. E., Chau, H. W., & Si, B. C. (2011). Impact of tension infiltrometer disc size on measured soil water repellency index. *Canadian Journal of Soil Science*, *91*(1), 77–81. https://doi.org/10.4141/cjss10033

Imeson, A. C., Verstraten, J. M., van Mulligen, E. J., & Sevink, J. (1992). The effects of fire and water repellency on infiltration and runoff under Mediterranean type forest. *Catena*, *19*(3–4), 345–361. https://doi.org/10.1016/0341-8162(92)90008-Y

Iovino, M., Pekárová, P., Hallett, P. D., Pekár, J., Lichner, Ľ., Mataix-Solera, J., … Rodný, M. (2018). Extent and persistence of soil water repellency induced by pines in different geographic regions. *Journal of Hydrology and Hydromechanics*, *66*(4), 360–368. https://doi.org/10.2478/johh-2018-0024

Jarvis, N., Etana, A., & Stagnitti, F. (2008). Water repellency, near-saturated infiltration and preferential solute transport in a macroporous clay soil. *Geoderma*, *143*(3–4), 223–230. https://doi.org/10.1016/j.geoderma.2007.11.015

de Jonge, L. W., Jacobsen, O. H., & Moldrup, P. (1999). Soil water repellency: effects of water content, temperature, and particle size. *Soil Science Society of America Journal*, *63*(3), 437–442. https://doi.org/10.2136/sssaj1999.03615995006300030003x

Lee, D. M., Reynolds, W. D., Elrick, D. E., & Clothier, B. E. (1985). A comparison of three field methods for measuring saturated hydraulic conductivity. *Canadian Journal of Soil Science*, *65*(3), 563–573. https://doi.org/10.4141/cjss85-060

Letey, J., Carrillo, M. L. K., & Pang, X. P. (2000). Approaches to characterize the degree of water repellency. *Journal of Hydrology*, *231–232*(0), 61–65. https://doi.org/10.1016/S0022-1694(00)00183-9

Lewis, S. A., Wu, J. Q., & Robichaud, P. R. (2006). Assessing burn severity and comparing soil water repellency, Hayman Fire, Colorado. *Hydrological Processes*, *20*(1), 1–16. https://doi.org/10.1002/hyp.5880

Lichner, L., Hallett, P. D., Drongová, Z., Czachor, H., Kovacik, L., Mataix-Solera, J., & Homolák, M. (2013). Algae influence the hydrophysical parameters of a sandy soil. *Catena*, *108*(0), 58–68. https://doi.org/10.1016/j.catena.2012.02.016

Moody, D. R., & Schlossberg, M. J. (2010). Soil water repellency index prediction using the molarity of ethanol droplet test. *Vadose Zone Journal*, *9*(4), 1046–1051. https://doi.org/10.2136/vzj2009.0119

Müller, K., Carrick, S., Meenken, E., Clemens, G., Hunter, D., Rhodes, P., & Thomas, S. (2016). Is subcritical water repellency an issue for efficient irrigation in arable soils? *Soil and Tillage Research*, *161*, 53–62. https://doi.org/10.1016/j.still.2016.03.010

Nelson, D. W., & Sommers, L. E. (1996). Total carbon, organic carbon and organic matter. In D. L. Sparks, A. L. Page, P. A. Helmke, & R. H. Loeppert (Eds.), *Methods of soil analysis. Part 3: Chemical methods* (pp. 961–1010). Madison, WI: Soil Science Society of America Inc.

Nyman, P., Sheridan, G., & Lane, P. N. J. (2010). Synergistic effects of water repellency and macropore flow on the hydraulic conductivity of a burned forest soil, south-east Australia. *Hydrological Processes*, *24*(20), 2871–2887. https://doi.org/10.1002/hyp.7701

Orfánus, T., Dlapa, P., Fodor, N., Rajkai, K., Sándor, R., & Nováková, K. (2014). How severe and subcritical water repellency determines the seasonal infiltration in natural and cultivated sandy soils. *Soil and Tillage Research*, *135*, 49–59. https://doi.org/10.1016/j.still.2013.09.005

Pekarova, P., Pekar, J., & Lichner, L. (2015). A new method for estimating soil water repellency index. *Biologia*, *70*(11), 1450–1455. https://doi.org/10.1515/biolog-2015-0178

Philip, J. R. (1957). The theory of infiltration: 1. The Infiltration equation and its solution. *Soil Science*, *83*(5), 345–358. https://doi.org/10.1097/00010694-195705000-00002

Robichaud, P. R., Lewis, S. A., & Ashmun, L. E. (2008). New procedure for sampling infiltration to assess post-fire soil water repellency. *Res. Note*. RMRS-RN-33. Rocky Mountain Station US: Department of Agriculture, Forest Service.

Schacht, K., Chen, Y., Tarchitzky, J., Lichner, L., & Marschner, B. (2014). Impact of treated wastewater irrigation on water repellency of Mediterranean soils. *Irrigation Science*, *32*(5), 369–378. https://doi.org/10.1007/s00271-014-0435-3

Sepehrnia, N., Hajabbasi, M. A., Afyuni, M., & Lichner, L. (2016). Extent and persistence of water repellency in two Iranian soils. *Biologia*, *71*(10), 1137–1143. https://doi.org/10.1515/biolog-2016-0135

Smettem, K. R. J., Parlange, J. Y., Ross, P. J., & Haverkamp, R. (1994). 3-dimensional analysis of infiltration from the disc infiltrometer. 1. A capillary-based theory. *Water Resources Research*, *30*(11), 2925–2929. https://doi.org/10.1029/94wr01787

Smettem, K. R. J., Ross, P. J., Haverkamp, R., & Parlange, J. Y. (1995). 3-dimensional analysis of infiltration from the disk infiltrometer. 3. Parameter-estimation using a double-disk tension infiltrometer. *Water Resources Research*, *31*(10), 2491–2495. https://doi.org/10.1029/95wr01722

Soil Survey Staff (2014). *Keys to soil taxonomy* ((12th edition ed.) ed.). Washington, DC: USDA-NRCS.

Tillman, R. W., Scotter, D. R., Wallis, M. G., & Clothier, B. E. (1989). Water-repellency and its measurement by using intrinsic sorptivity. *Australian Journal of Soil Research*, *27*(4), 637–644. https://doi.org/10.1071/Sr9890637

Vandervaere, J.-P., Vauclin, M., & Elrick, D. E. (2000a). Transient flow from tension infiltrometers. I. The two-parameter equation. *Soil Science Society of America Journal*, *64*(4), 1263–1272. https://doi.org/10.2136/sssaj2000.6441263x

Vandervaere, J.-P., Vauclin, M., & Elrick, D. E. (2000b). Transient flow from tension infiltrometers. II. Four methods to determine sorptivity and conductivity. *Soil Science Society of America Journal*, *64*(4), 1272–1284. https://doi.org/10.2136/sssaj2000.6441272x

Van't Woudt, B. D. (1959). Particle coatings affecting the wettability of soils. *Journal of Geophysical Research*, *64*(2), 263–267. https://doi.org/10.1029/JZ064i002p00263

Vogelmann, E. S., Reichert, J. M., Prevedello, J., Consensa, C. O. B., Oliveira, A. É., Awe, G. O., & Mataix-Solera, J. (2013). Threshold water content beyond which hydrophobic soils become hydrophilic: The role of soil texture and organic matter content. *Geoderma*, *209–210*(0), 177–187. https://doi.org/10.1016/j.geoderma.2013.06.019

Watson, C. L., & Letey, J. (1970). Indices for characterizing soil-water repellency based upon contact angle-surface tension relationships. *Soil Science Society of America Proceed`ings*, *34*(6), 841–844. https://doi.org/10.2136/sssaj1970.03615995003400060011x

**How to cite this article:** Alagna V, Iovino M, Bagarello V, Mataix-Solera J, Lichner L. Alternative analysis of transient infiltration experiment to estimate soil water repellency. *Hydrological Processes*. 2019;33:661–674. https://doi.org/10.1002/hyp.13352